



Supplement of

Overestimation of closed-chamber soil CO₂ effluxes at low atmospheric turbulence

Andreas Brændholt et al.

Correspondence to: Andreas Brændholt (andbr@env.dtu.dk)

The copyright of individual parts of the supplement might differ from the CC-BY 3.0 licence.

Information

The following document contains the results from the linearly and non-linearly calculated soil CO₂ effluxes at four different dead bands of 10, 20, 30 and 40 seconds.

Figure 1-8 show the seasonally averaged diurnal patterns of soil CO₂ effluxes at different friction velocity (u_*) threshold values for effluxes calculated at a specific dead band and calculation method. These figures use the same template as Fig. 5 in the manuscript, and Fig. 2 (linearly calculated at dead band 20) is identical to Fig. 5 in the manuscript.

Fig. 9 shows the calculated annual soil CO₂ effluxes for each dead band and flux calculation method. It is an extended version of Fig. 7 in the manuscript.

10

15

20

Linearly calculated soil CO₂ effluxes at 10 s dead band

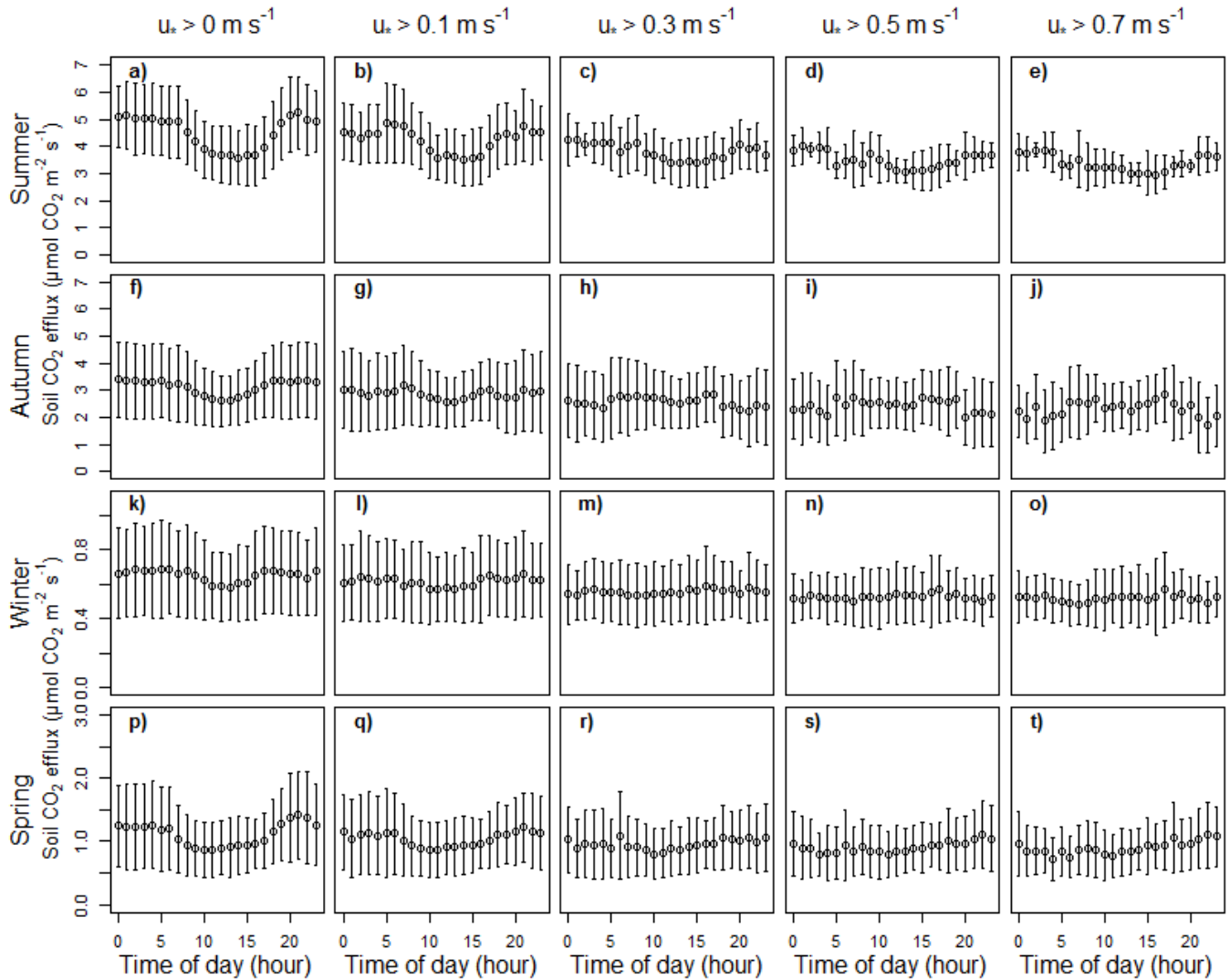


Figure 1: Seasonally averaged diurnal patterns of soil CO₂ efflux (\pm standard deviation), at different friction velocity (u_*) threshold values, measured by the eight automated chambers for each of the 4 seasons. Effluxes are linearly calculated at a dead band of 10 s. From the top, the four rows show the diurnal patterns for summer, autumn, winter and spring respectively. From the left, the five columns show the diurnal patterns for each season at no u_* filtering, a u_* threshold value of 0.1 m s^{-1} , a u_* threshold value of 0.3 m s^{-1} , a u_* threshold value of 0.5 m s^{-1} and a u_* threshold value of 0.7 m s^{-1} , respectively.

Linearly calculated soil CO₂ effluxes at 20 s dead band

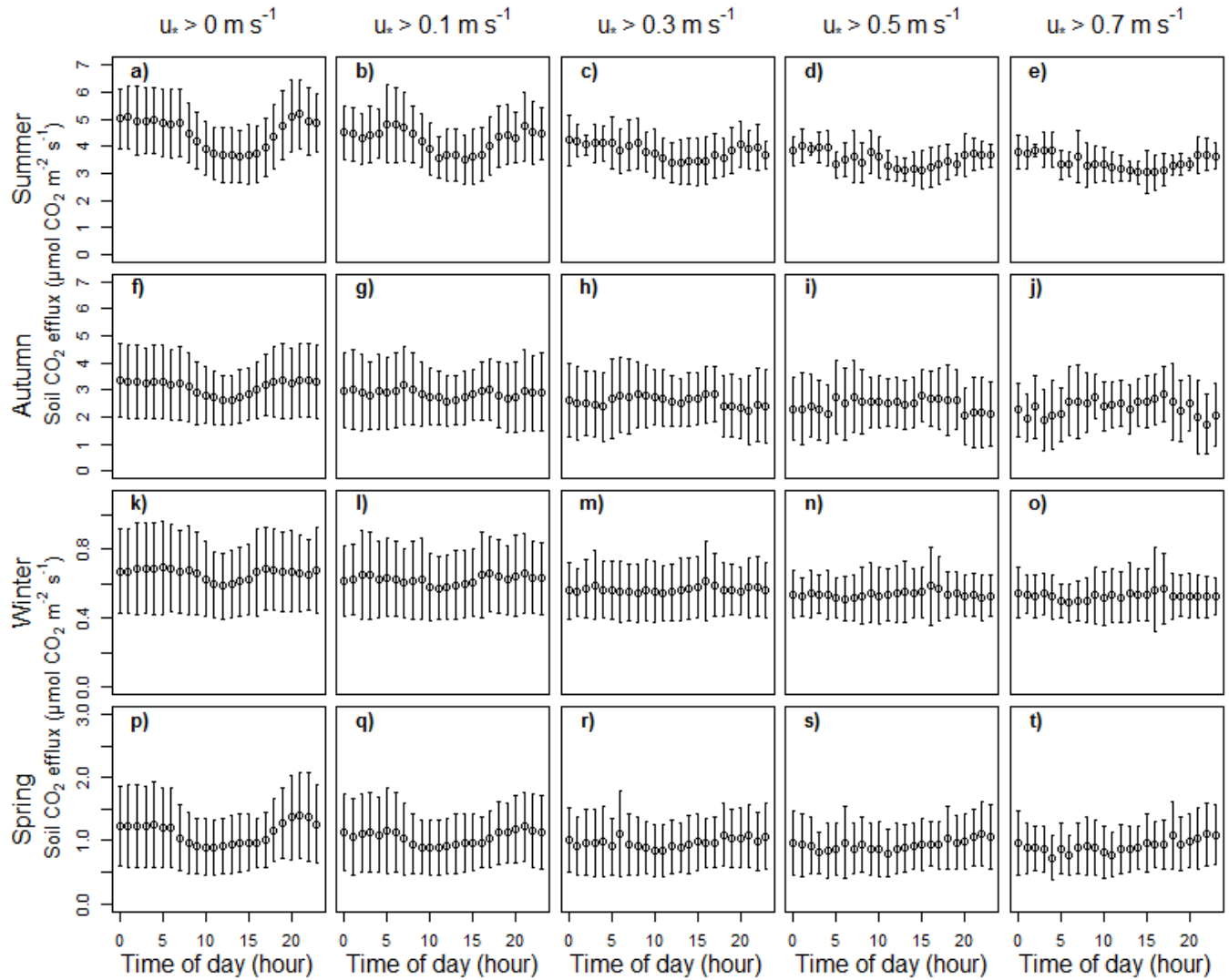


Figure 2: Seasonally averaged diurnal patterns of soil CO₂ efflux (\pm standard deviation), at different friction velocity (u_*) threshold values, measured by the eight automated chambers for each of the 4 seasons. Effluxes are linearly calculated at a dead band of 20 s. From the top, the four rows show the diurnal patterns for summer, autumn, winter and spring respectively. From the left, the five collars show the diurnal patterns for each season at no u_* filtering, a u_* threshold value of 0.1 m s^{-1} , a u_* threshold value of 0.3 m s^{-1} , a u_* threshold value of 0.5 m s^{-1} and a u_* threshold value of 0.7 m s^{-1} , respectively.

Linearly calculated soil CO₂ effluxes at 30 s dead band

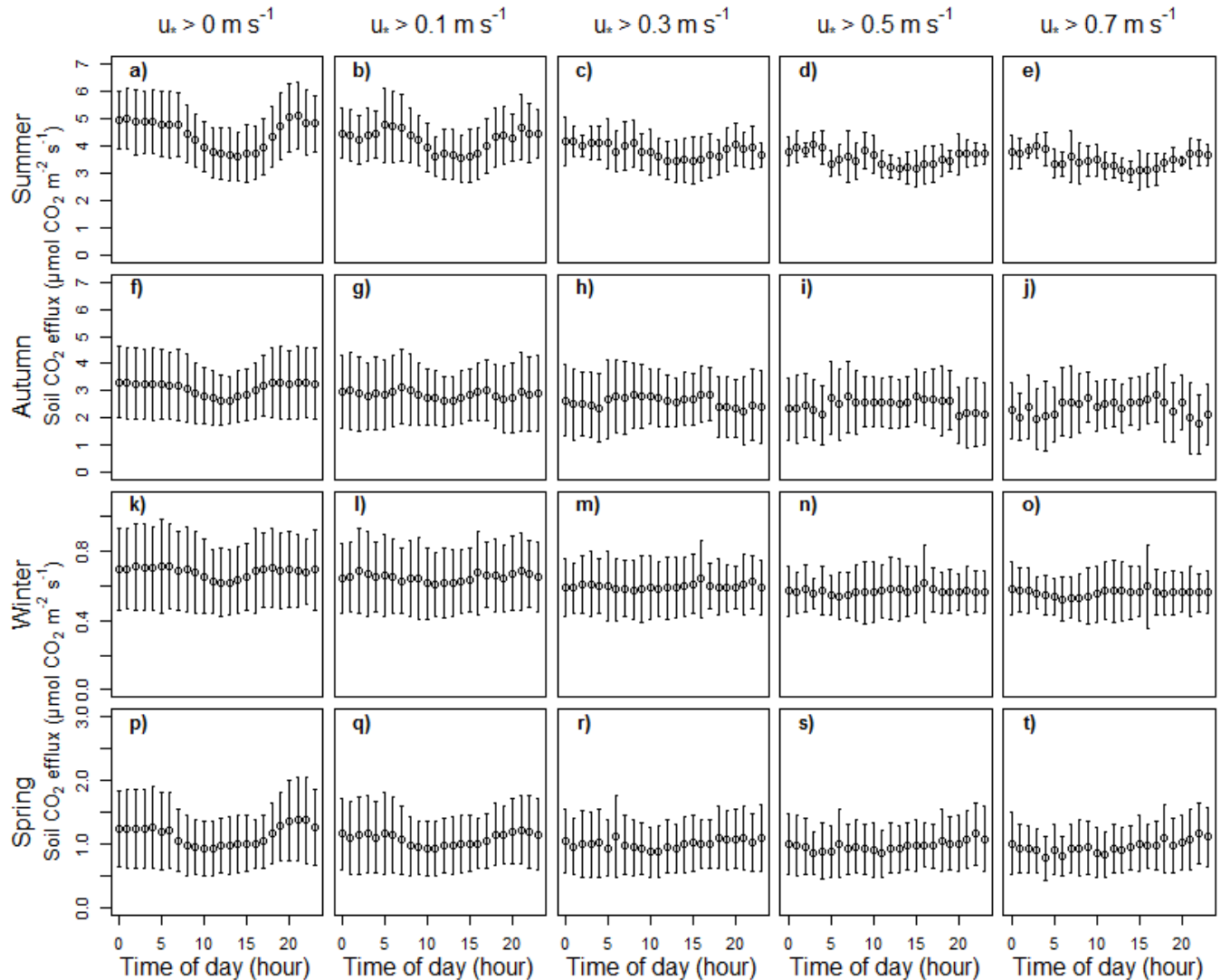


Figure 3: Seasonally averaged diurnal patterns of soil CO₂ efflux (\pm standard deviation), at different friction velocity (u_*) threshold values, measured by the eight automated chambers for each of the 4 seasons. Effluxes are linearly calculated at a dead band of 30 s. From the top, the four rows show the diurnal patterns for summer, autumn, winter and spring respectively. From the left, the five collars show the diurnal patterns for each season at no u_* filtering, a u_* threshold value of 0.1 m s^{-1} , a u_* threshold value of 0.3 m s^{-1} , a u_* threshold value of 0.5 m s^{-1} and a u_* threshold value of 0.7 m s^{-1} , respectively.

5

Linearly calculated soil CO₂ effluxes at 40 s dead band

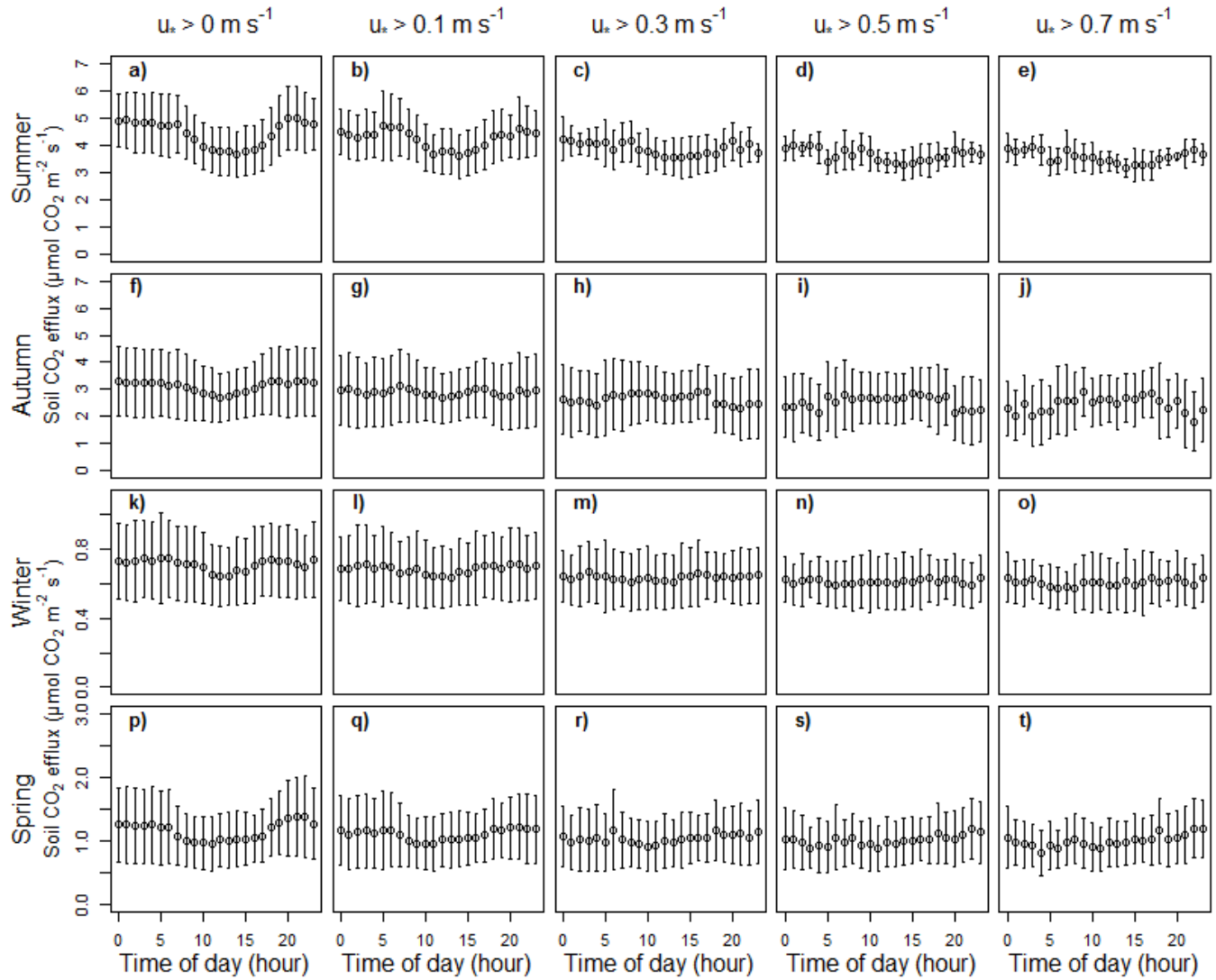
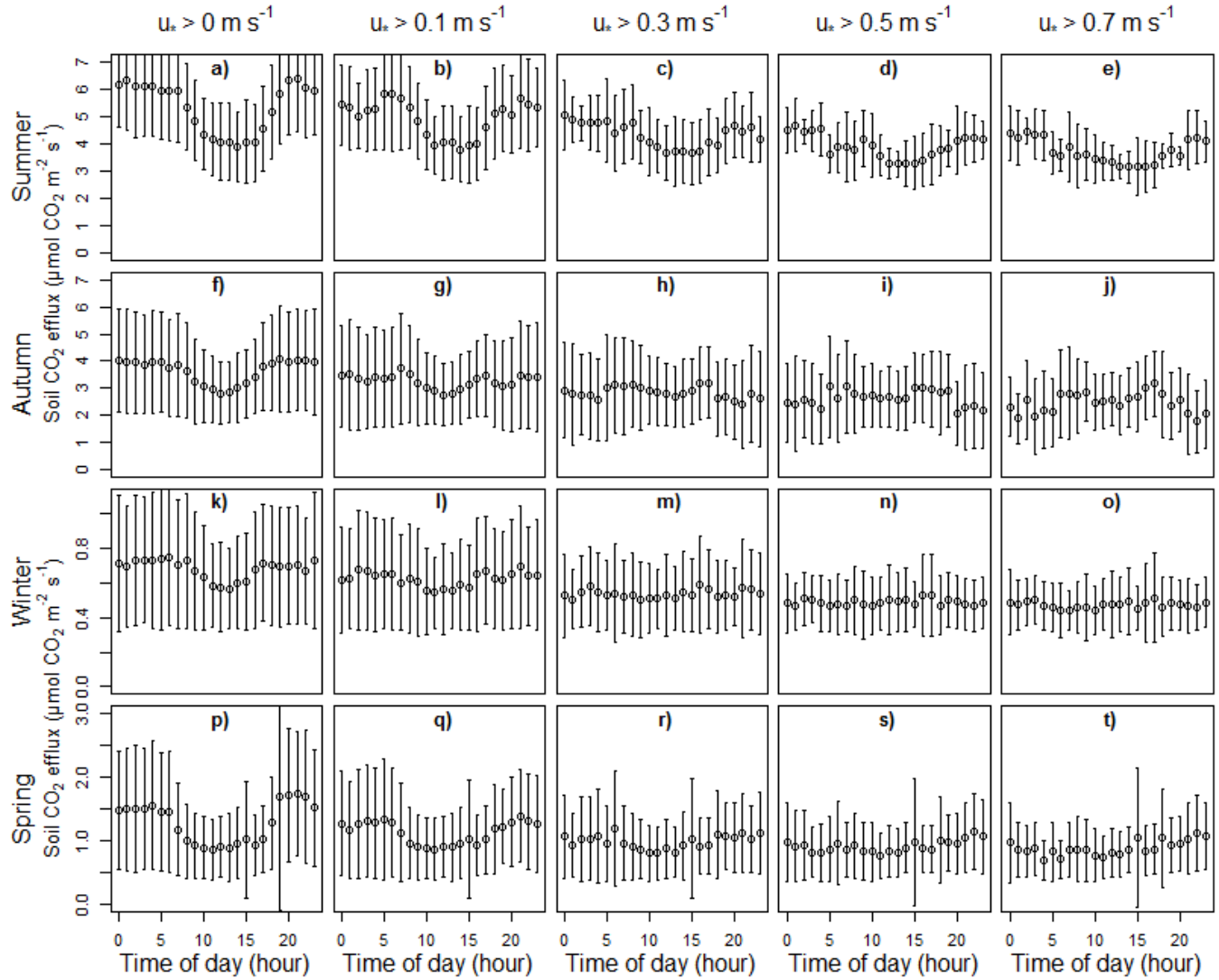


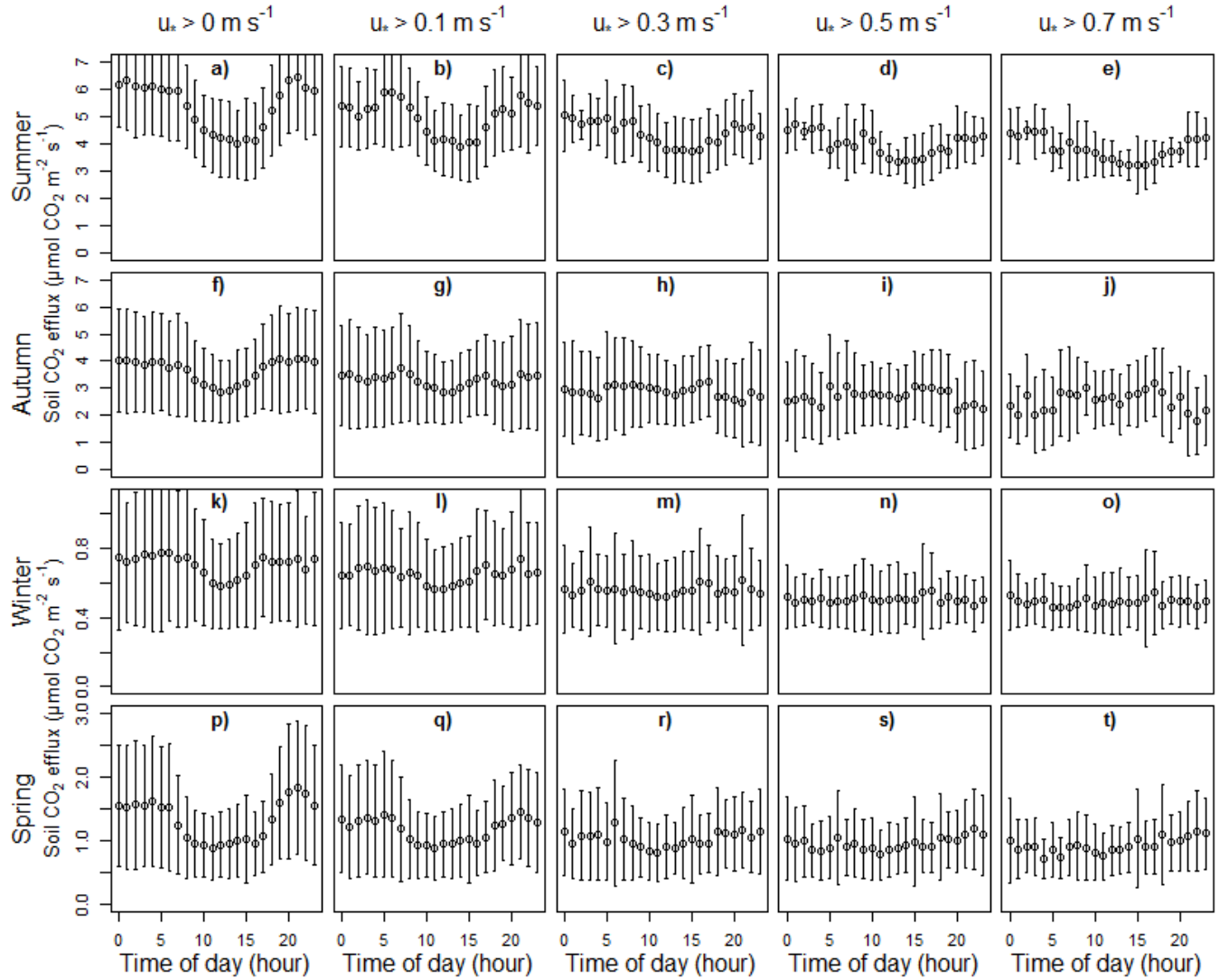
Figure 4: Seasonally averaged diurnal patterns of soil CO₂ efflux (\pm standard deviation), at different friction velocity (u_*) threshold values, measured by the eight automated chambers for each of the 4 seasons. Effluxes are linearly calculated at a dead band of 40 s. From the top, the four rows show the diurnal patterns for summer, autumn, winter and spring respectively. From the left, the five collars show the diurnal patterns for each season at no u_* filtering, a u_* threshold value of 0.1 m s^{-1} , a u_* threshold value of 0.3 m s^{-1} , a u_* threshold value of 0.5 m s^{-1} and a u_* threshold value of 0.7 m s^{-1} , respectively.

Non-linearly calculated soil CO₂ effluxes at 10 s dead band



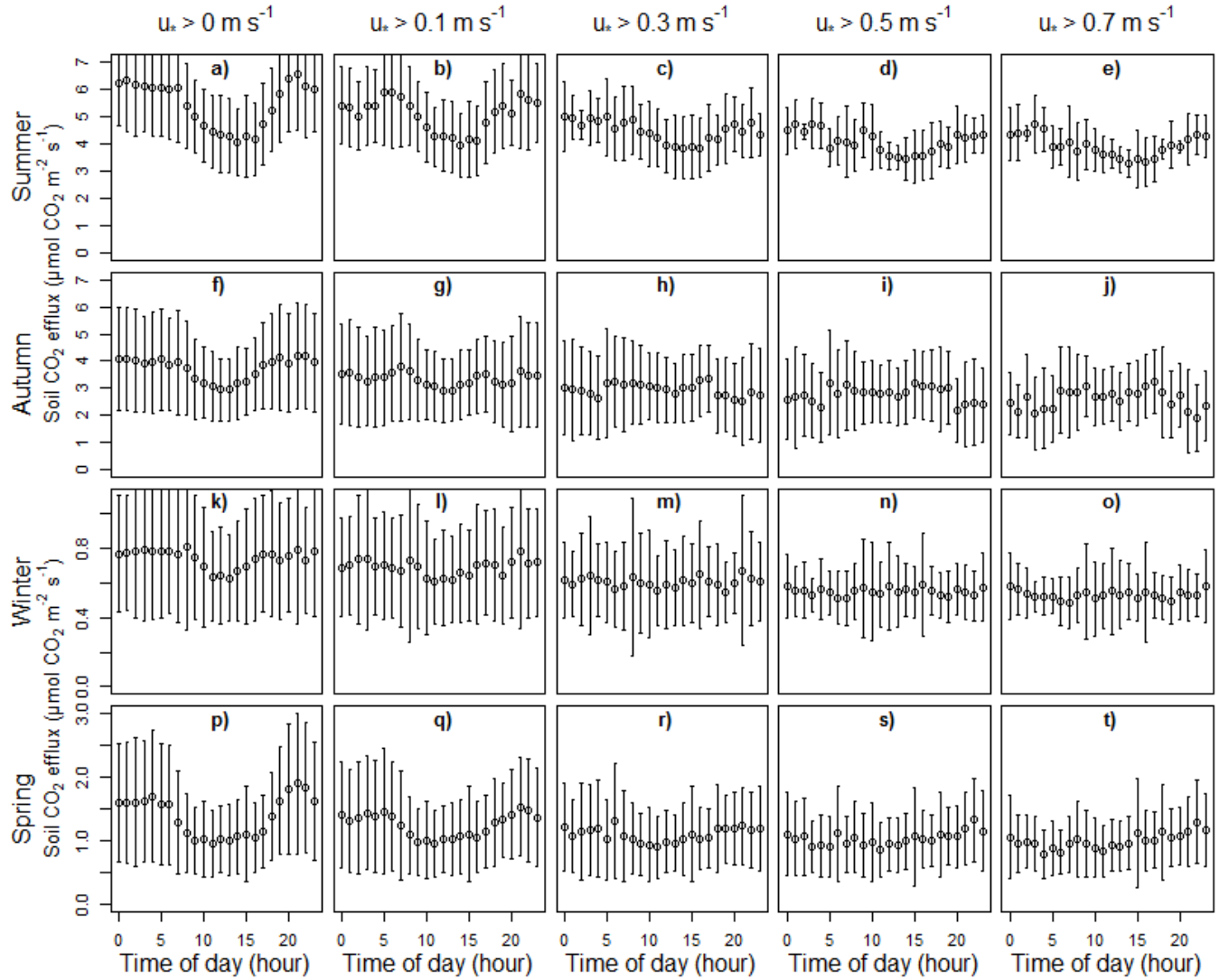
5 **Figure 5:** Seasonally averaged diurnal patterns of soil CO₂ efflux (\pm standard deviation), at different friction velocity (u_*) threshold values, measured by the eight automated chambers for each of the 4 seasons. Effluxes are non-linearly calculated at a dead band of 10 s. From the top, the four rows show the diurnal patterns for summer, autumn, winter and spring respectively. From the left, the five collars show the diurnal patterns for each season at no u_* filtering, a u_* threshold value of 0.1 m s^{-1} , a u_* threshold value of 0.3 m s^{-1} , a u_* threshold value of 0.5 m s^{-1} and a u_* threshold value of 0.7 m s^{-1} , respectively.

Non-linearly calculated soil CO₂ effluxes at 20 s dead band



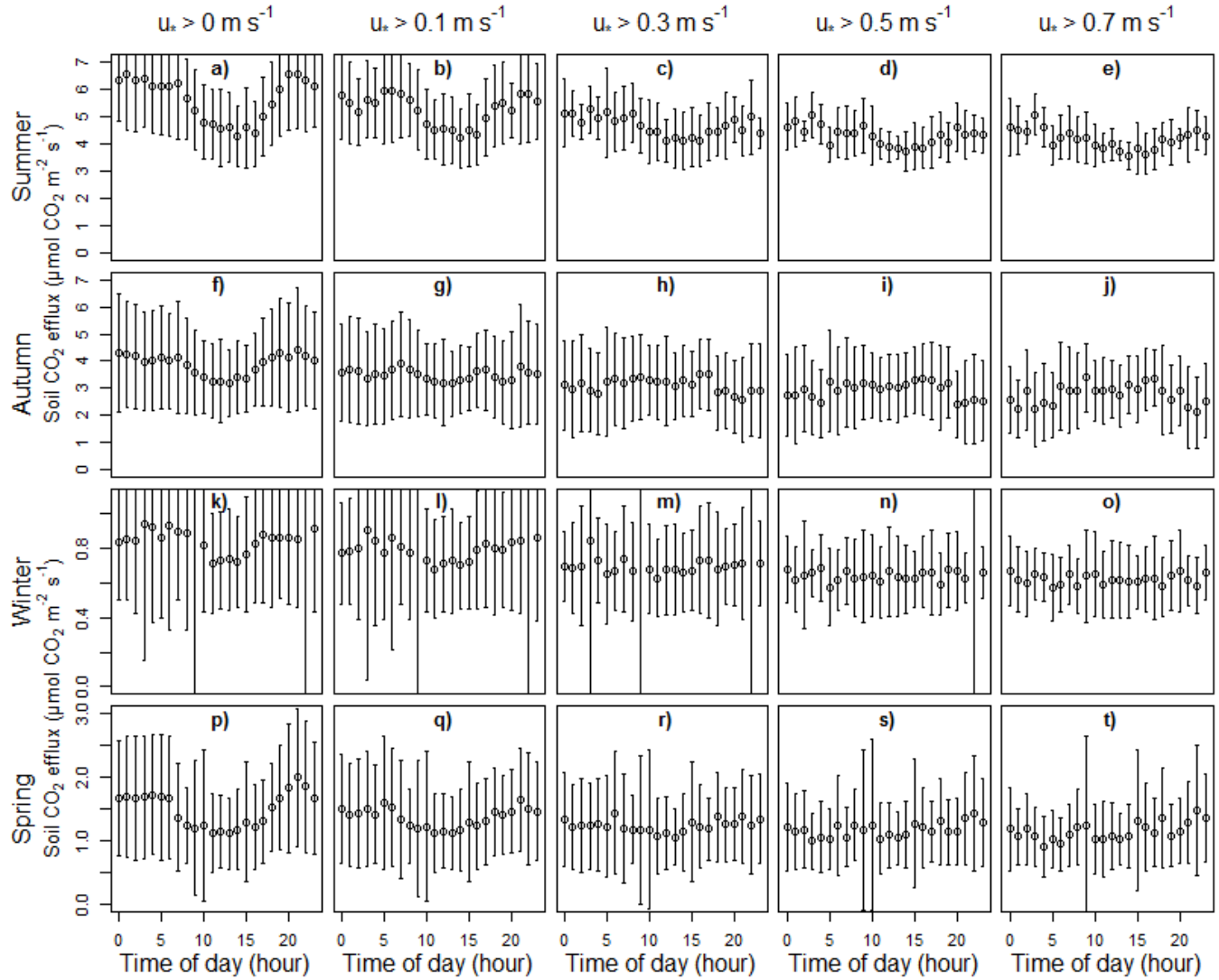
5 **Figure 6:** Seasonally averaged diurnal patterns of soil CO₂ efflux (\pm standard deviation), at different friction velocity (u_*) threshold values, measured by the eight automated chambers for each of the 4 seasons. Effluxes are non-linearly calculated at a dead band of 20 s. From the top, the four rows show the diurnal patterns for summer, autumn, winter and spring respectively. From the left, the five collars show the diurnal patterns for each season at no u_* filtering, a u_* threshold value of 0.1 m s^{-1} , a u_* threshold value of 0.3 m s^{-1} , a u_* threshold value of 0.5 m s^{-1} and a u_* threshold value of 0.7 m s^{-1} , respectively.

Non-linearly calculated soil CO_2 effluxes at 30 s dead band



5 **Figure 7:** Seasonally averaged diurnal patterns of soil CO_2 efflux (\pm standard deviation), at different friction velocity (u_*) threshold values, measured by the eight automated chambers for each of the 4 seasons. Effluxes are non-linearly calculated at a dead band of 30 s. From the top, the four rows show the diurnal patterns for summer, autumn, winter and spring respectively. From the left, the five collars show the diurnal patterns for each season at no u_* filtering, a u_* threshold value of 0.1 m s^{-1} , a u_* threshold value of 0.3 m s^{-1} , a u_* threshold value of 0.5 m s^{-1} and a u_* threshold value of 0.7 m s^{-1} , respectively.

Non-linearly calculated soil CO₂ effluxes at 40 s dead band



5 **Figure 8:** Seasonally averaged diurnal patterns of soil CO₂ efflux (\pm standard deviation), at different friction velocity (u_*) threshold values, measured by the eight automated chambers for each of the 4 seasons. Effluxes are non-linearly calculated at a dead band of 40 s. From the top, the four rows show the diurnal patterns for summer, autumn, winter and spring respectively. From the left, the five collars show the diurnal patterns for each season at no u_* filtering, a u_* threshold value of 0.1 m s^{-1} , a u_* threshold value of 0.3 m s^{-1} , a u_* threshold value of 0.5 m s^{-1} and a u_* threshold value of 0.7 m s^{-1} , respectively.

Calculated annual soil CO₂ effluxes

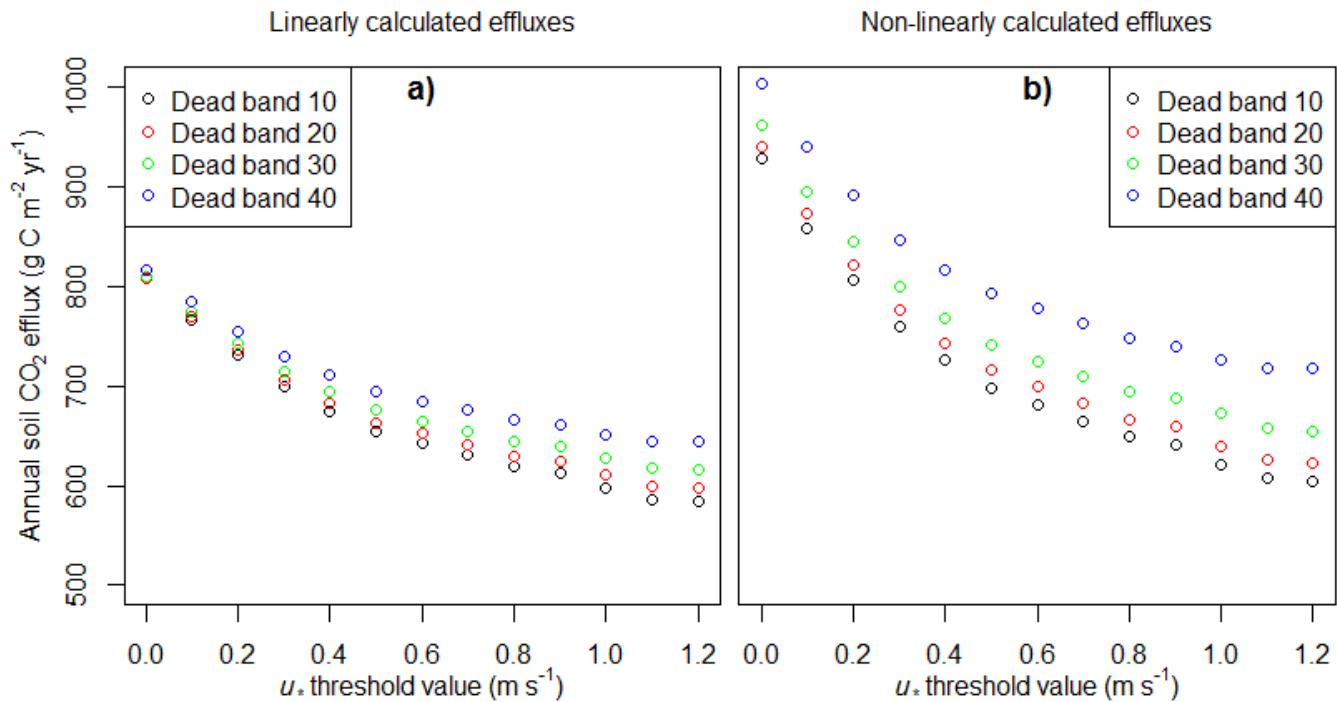


Figure 9: Calculated annual soil CO₂ effluxes in response to increasing the friction velocity (u_*) threshold values for the automated chamber measurements during the one year campaign. (a) shows annual soil CO₂ effluxes for the linearly calculated effluxes at four different dead bands. (b) shows annual soil CO₂ effluxes for the non-linearly calculated effluxes at four different dead bands.